Catalysis Today 146 (2009) 230–233

Contents lists available at ScienceDirect

Catalysis Today

journal homepage: www.elsevier.com/locate/cattod

Structural characterization and effect of dehydration on the Ni-doped titanate nanotubes

Dong Hyun Kim [a,*], Jum Suk Jang [b], Nam Hoon Goo [a], Min Serk Kwon [c], Jin Woo Lee [d], Sun Hee Choi [e], Dong Wook Shin [a], Sun-Jae Kim [f], Kyung Sub Lee [a]

[a] Division of Materials Science & Engineering, Hanyang University, 133-791 Seoul, Republic of Korea
[b] Department of Chemistry and Biochemistry, The University of Texas at Austin, Austin, TX 78712, United States
[c] Department of Chemistry, Pohang University of Science and Technology, Pohang 790-784, Republic of Korea
[d] Department of Mechanical Engineering, Choongnam University, Yuseong-gu, Daejeon 305-764, Republic of Korea
[e] Pohang Accelerator Laboratory, Beamline Research Division, Pohang 790-784, Republic of Korea
[f] Institute/Faculty of Nanotechnology and Advanced Materials Engineering, Sejong University, 98 Gunja-dong, Gwangjin-gu, Seoul 143-747, Republic of Korea

ARTICLE INFO

Article history:
Available online 23 May 2009

Keywords:
Titanate nanotubes
Hydrothermal method
Hydrogen storage
XFAS
Ni dopant

ABSTRACT

Titanate nanotubes and Ni-doped titanate nanotubes were synthesized by hydrothermal method and simple firing using rutile powders as starting materials. The hydrogen absorption of the nanotubes was investigated by the conventional volumetric pressure–composition (*P–C*) isothermal method using an automated Sivert's type apparatus. The microstructure and morphology of the synthesized nanotubes were characterized by X-ray diffraction (XRD), high resolution transmission electron microscopy (HR-TEM). Titanate nanotubes compose of $H_2Ti_2O_5{\cdot}H_2O$ in accordance with DFT (Density Functional Theory) calculation and has outer and inner diameter of ~10 and 6 nm, and the interlayer spacing about 0.65–0.74 nm. The storage capacity of hydrogen in the Ni-doped nanotubes increased linearly with pressure and revealed reliable evidence of hydrogen sorption at room temperatures.

1. Introduction

One dimensional titania have been extensively studied for photocatalysis, dye-sensitized solar cell, lithium ion batteries, hydrogen storage, and electrochemical capacitors [1–5] due to its large specific surface area, numerous surface defects and physicochemical potentials [6–9]. Specially, there have been reports to apply titanate nanotubes for hydrogen storage, however, absorbing reaction occurred only at high temperature and/or low temperature (at −196 °C and over 120 °C) [10]. Bavykin et al. reported that the hydrogen could be intercalate between layers in the walls of TiO_2 nanotubes forming host–guest compounds $TiO_2{\cdot}xH_2$, where $x \leq 1.5$ and decreases at higher temperatures [11]. Also, the TiO_2 nanotubes by Lim et al. showed that about 2 wt% hydrogen could be reproducibly stored at room temperature and 6 MPa [10]. However, in spite of these efforts, much work on the characterizations of structural and hydrogen absorption of titanate nanotubes are required. Also, systematic study on dehydration of nanotubes and interlayer spacing has yet to be done. Most researchers reported that the crystal structures of the titanate nanotubes have $A_2Ti_3O_7$, $H_2Ti_4O_9{\cdot}H_2O$ (A = Na and/or H), and lepidocrocite titanates with monoclinic crystal structure [12–14]. However, the corresponding of XRD patterns was not fully coincided with the crystal structure from JCPDS (Joint Committee on Power Diffraction Standards).

In our previous work, Ni-doped titanate nanotubes were synthesized by hydrothermal method using Ni-doped TiO_2 rutile powders and demonstrated exact crystal structure of the nanotubes (Ni-doped $H_2Ti_2O_5{\cdot}H_2O$) [15]. However, nanotubes had lots of hydrate in the crystal and on the surface which acted as a brake on hydrogen absorbing. In this work, Ni-doped titanate nanotubes were synthesized by hydrothermal method and simple firing and effect of dehydration on the Ni-doped titanate nanotubes for hydrogen storage was studied. And the crystal structures of synthesized nanotubes have been discussed. Also, the hydrogen absorption of nanotube was investigated by the conventional volumetric pressure–composition (*P–C*) isothermal method using an automated Sivert's type apparatus.

2. Experimental

The Ni-doped powders (0.8 g) and 15 mL of a 10 M NaOH aqueous solution were mixed with stirring for 1 h and placed in a Ni-lined stainless-steel autoclave at 120 °C for 24 h, and then

* Corresponding author. Tel.: +82 2 2281 4914; fax: +82 2 2281 4914.
E-mail address: dhk@hanyang.ac.kr (D.H. Kim).

0920-5861/$ – see front matter © 2009 Elsevier B.V. All rights reserved.
doi:10.1016/j.cattod.2009.04.007

cooled at room temperature. Next, 0.1 M HCl aqueous solution was added and washed repeatedly with distilled water until pH 7. Final powders were collected by the centrifugal separator (Oak redge tube) which operated at 15,000 rpm for 30 min. After then, the synthesized powders are heated at 450 and 600 °C for 2 h in to check the effect of firing. The microstructure and morphology of the synthesized powders were characterized by X-ray diffraction (XRD: Rigaku-denki D/max2500) using Cu Kα (λ = 1.5418 Å), high resolution transmission electron microscope (HRTEM: JEOL4010) with accelerating voltage of 400 kV, and the thermogravimetric measurement was made using a TG-DTA (Differential thermal-gravimetric analysis) instrument.

The electronic geometric structures around Ti and Ni in the materials were characterized with X-ray absorption fine structure (XAFS). X-ray absorption measurements were conducted at beamline 3C1 of PAL (Pohang Accelerator Laboratory) (2.5 GeV; stored current of 130–180 mA), The radiation was monochromatized using a Si(1 1 1) double crystal monochromator and the incident beam was detuned by 15–30% using a piezo-electric translator in order to minimize contamination from higher harmonics, in particular, the 3rd order reflection of the silicon crystals. Data were collected at room temperature in transmission mode. The intensities of incident and transmitted beams were measured by ionization chamber detectors where N_2 gas flowed. The energy was calibrated by measuring X-ray absorption spectrum of Ni and Ti metal foil and by assigning the first inflection point in the rising portion of the absorption spectra as 8333 and 4966 eV, respectively. The obtained data were analyzed using IFEFFIT (interactive program for analysis of x-ray absorption spectroscopy data) suite of software programs [16]. The hydrogen absorption tests were conducted by the conventional volumetric pressure–composition (*P*–*C*) isothermal method using an automated Sivert's type apparatus. 5 g of the synthesized samples were loaded into a steel reactor and hydrogen gas (purity: 99.9999%) at a pressure of 20 atm was introduced after an initial dehydriding for 20 h in a vacuum at room temperature for hydrogen absorption.

3. Results and discussion

Fig. 1 shows the XRD patterns of the Ni-doped titanate nanotubes (TNT) and fired Ni-doped titanate nanotubes with the reported crystal structure from JCPDS [9,17,18]. The Ni-doped TNT and fired TNT at 400 °C powders revealed characteristic peaks at around $2\theta = 10°$, 24°, and 28° which could be assigned to the diffraction of $H_2Ti_2O_5{\cdot}H_2O$ with peak broadening that was the result of nanometer size and bending of some atom planes of the tubes [11]. Also, Ni element peaks were not detected in the patterns as Ni was fully dissolved in the nanotubes. However, the main peaks of the Ni TNT and fired TNT were slightly different due to the dehydration by firing. Calculating d_{200} and d_{110} value from XRD patterns indicated that the interlayer spacing of the Ni-doped TNT and the fired TNT from the reflection (2 0 0) were 0.91 and 0.84 nm, respectively. It can be seen that the crystal structures of the synthesized nanotubes were completely different from those reported by other researchers [12–14] in spite of the similar morphologies of nanotubes.

Fig. 2 shows the HRTEM images of the Ni-doped TNT (a) and fired TNT (b). The nanotubes have multiple layers of 4–5 with the interlayer spacing of 0.74 and 0.65 nm, respectively. And the diameters of the nanotubes were almost 6–10 nm which had the length of several tens to hundred nanometers with all open at both ends. The difference of the interlayer spacing between Ni-doped TNT and fired TNT may be due to elimination of structural and absorbing water in the nanotubes during firing. The axis of the nanotubes was [0 0 1] direction, and the layer stacking was parallel to the axis. The selected area electron diffraction (SAED) patterns

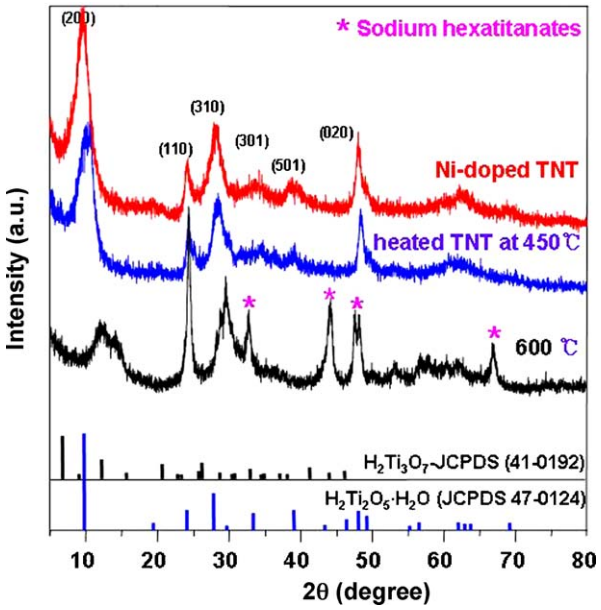

Fig. 1. XRD patterns of Ni-doped nanotubes, and fired titanate nanotubes at 450, 600 °C. The standard diffraction peaks are indexed according to $H_2Ti_2O_5{\cdot}H_2O$, $H_2Ti_3O_7$, and $Na_2Ti_3O_7$ from JCPDS.

exhibited that both patterns indicate diffraction lines of hydrogen titanate hydrate, (2 0 0), (1 1 0), (3 1 0), (5 0 1), (0 2 0), except small distortion in Ni-doped nanotubes by doping. The typical EDS (Energy Dispersive Spectrometer) data collected from the average over five different points of analysis in Ni-doped nanotubes exhibited that the Ni-doped nanotubes contained about 7 wt% Ni. On the other hand, when the firing temperature was over at 450 °C, the morphology of the nanotubes changed to nanosheet and/or nanoplate due to excess dehydration.

The dehydration of trapped water in the Ni-doped nanotubes was monitored by thermogravimetric analysis and the result is

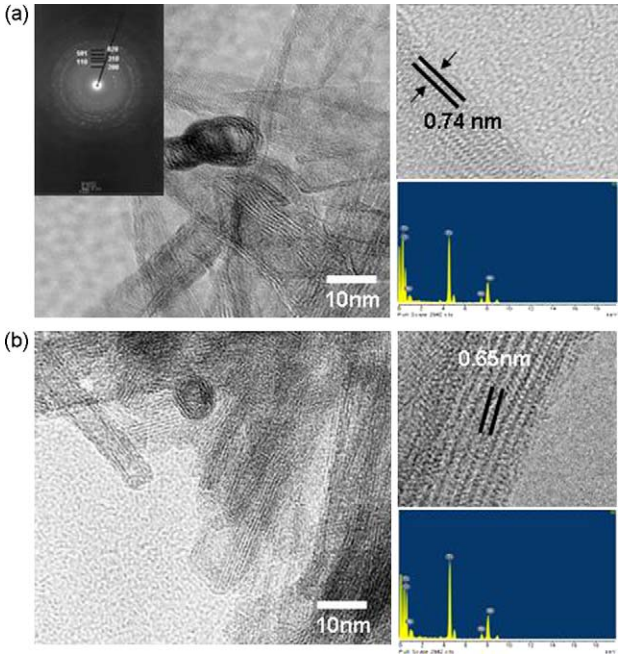

Fig. 2. (a) High resolution TEM image of the Ni-doped nanotubes. (b) High resolution TEM image of the fired nanotube with EDS analysis and selected diffraction patterns. The selected diffraction patterns of the center area of the nanotube.

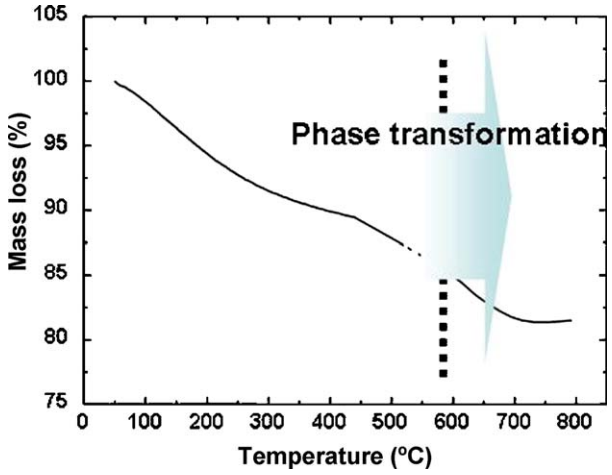

Fig. 3. Thermogravimetric diagram of the Ni-doped nanotubes. The temperature sloping rate is 10 °C/min.

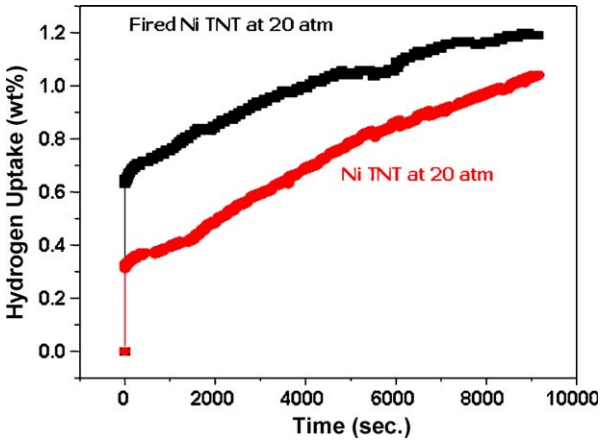

Fig. 5. Hydrogen absorption curves of the nanotubes at 30 °C both Ni-doped TNT and fired TNT.

shown in Fig. 3. The weight loss of the Ni-doped nanotubes was about 11.2 wt% after heating until 450 °C and revealed a weight loss about 13 wt% at 600 °C. Generally, the weight loss of titanate nanotubes strongly depend on the temperature and time for drying or different washing times, because of strong water-absorbent capability by the capillarity in the nanotubes [19,20]. It means that large parts of hydrate in the nanotubes were decreased by firing process although the nanotubes contained less hydrates.

Fig. 4 shows Ti K-edge X-ray Absorption Near-Edge Structure (XANES) (a) and Ni K-edge XANES (b) of the undoped nanotubes and Ni-doped nanotubes. Three weak peaks at 4966–4974 eV in Fig. 4(a) are indicative of the forbidden transitions from the core 1s level to the unoccupied 3d states of Ti^{4+} in the distorted TiO^6 octahedron [21,22]. The characteristic peaks of octahedral symmetry have been sometimes observed as four peaks depending on energy resolution [23]. The similar pre-edge structures before and after Ni-doping could be a direct evidence that the nickels are not substituted into the lattice of TiO_6 octahedron in $H_2Ti_2O_5{\cdot}H_2O$. It is also supported by similar features above 4980 eV having only slight difference in the intensity of the oscillation. The Fourier transforms of the Ti K-edge of

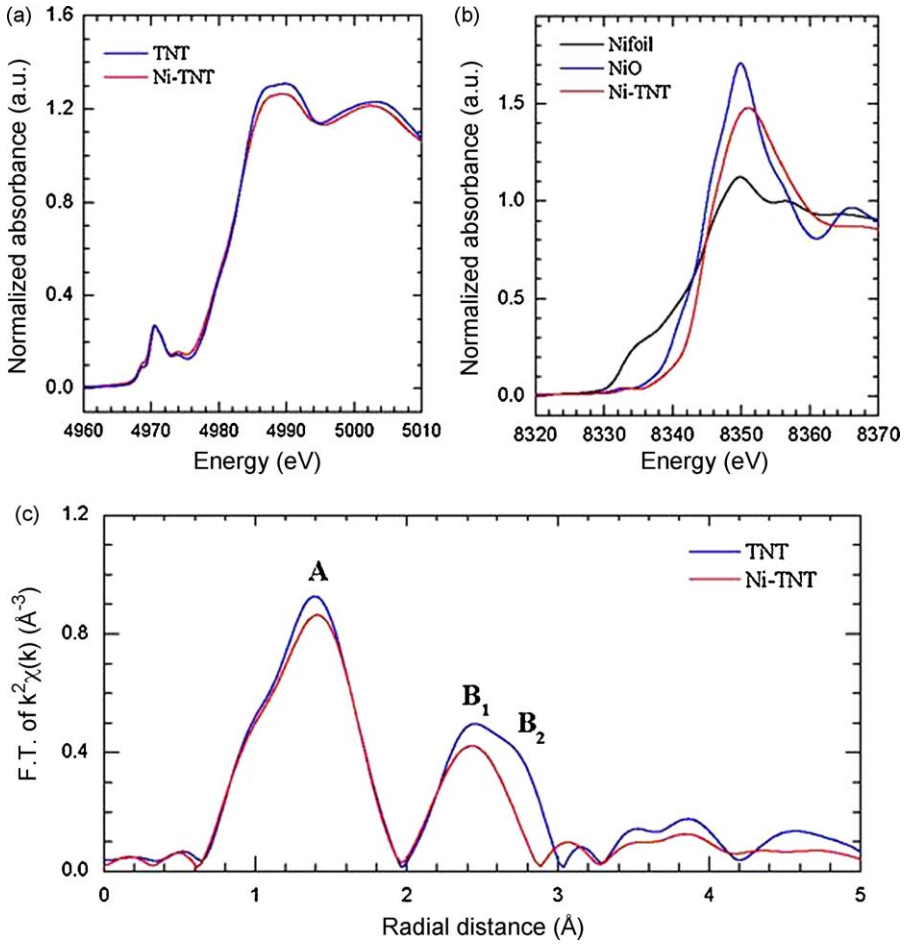

Fig. 4. Ti K-edge XANES (a) and Ni K-edge XANES (b), and the Fourier transforms of Ti K-edge (c) of the undoped (TNT) and Ni-doped nanotubes (Ni-TNT).

the undoped and Ni-doped nanotubes are shown in Fig. 4(c). The peak *A* at 0.6–2.0 Å which can be assigned as Ti-O scatterings are similar in both samples, but the shoulder peak B_2 at 2–3 Å disappeared in the Ni-doped nanotubes. In the case of $H_2Ti_2O_5{\cdot}H_2O$ H_2O structure, Ti would have two types of surrounding titanium atoms, one from in-layer TiO_6 octahedron and the other from out-of-layer octahedron. Since the two have different bond lengths of Ti–Ti because of the interlayering H^+, two peaks B_1 and B_2 are clearly observed in the undoped nanotubes. When nickel would exits in the interlayer of the nanotubes as mentioned in the XRD analysis, the interlayer spacing are increased and consequently the scattering from Ti in TiO_6 octahedron at the out-of-layer has little influence on the Ti at the in-layer. It leads to a conclusion that the doped nickels are placed between the lattices of TiO_6 octahedron, not replaced with the Ti atom in the lattice. In order to investigate the chemical state of the Ni dopant in nanotubes, Ni K-edge XANES of the sample was compared with Ni metal and NiO (Fig. 4(b)). The feature of Ni-doped nanotubes is distinctly different from that of Ni metal and its absorption edge is shifted to a higher energy than NiO. The Ni K-edge of the sample is almost as that of $Ni_2O_3{\cdot}H_2O$ in the reference [24]. XANES results strongly suggest that Ni should exits as a trivalent state in the nanotubes due to the substitution of Ni^{3+} instead of $3H^+$.

The hydrogen absorption was measured at 30 °C with on Ni-doped TNT and fired TNT nanotubes and these results are shown in Fig. 5. The Ni-doped and fired TNT revealed that the hydrogen absorption capacity of fired TNT was 1.21 wt% at 30 °C, 20 atm while the hydrogen capacity of Ni-TNT was 1.03 wt%. As mentioned previously, Ni dopant could give easy path to hydrogen diffusion so that the absorbed hydrogen could be stored in the interlayers of titanate nanotubes [25]. On the other hand, the absorption site of the hydrogen in titanate nanotubes is not clarified yet, however, the hydrogen could not easily adsorbed to the titanate nanotubes due to lots of hydrate. Therefore, fired TNT revealed higher hydrogen absorption capacity than that of the Ni TNT which was caused by elimination of the absorbed hydrate during simple firing.

4. Conclusion

Ni-doped titanate nanotube and Ni-doped nanotubes were synthesized by hydrothermal method and simple firing using rutile powders as starting materials. The hydrogen absorption of the nanotubes was investigated by the conventional volumetric pressure–composition (*P*–*C*) isothermal method using an automated Sivert's type apparatus.

The nanotubes compose of $H_2Ti_2O_5{\cdot}H_2O$ with outer and inner diameter of ~10 and 6 nm, and the interlayer spacing is about 0.65–0.74 nm which were totally different from the other results as previously reported. The storage capacity of hydrogen in the Ni-doped nanotubes increased linearly with firing and revealed reliable evidence of hydrogen sorption at room temperatures.

References

[1] H. Zhang, G.R. Li, L.P. An, T.Y. Yan, X.P. Gao, H.Y. Zhu, J. Phys. Chem. C 111 (2007) 6143.
[2] J. Li, Z. Tang, Z. Zhang, Electrochem. Commun. 7 (2005) 62.
[3] J. Li, Z. Tang, Z. Zhang, Chem. Mater. 17 (2005) 5848.
[4] F. Cheng, J. Chen, J. Mater. Res. 21 (2006) 2744.
[5] L. Kavan, M. Kalbac, M. Zukalova, I. Exnar, V. Lorenzen, R. Nesper, M. Graetzel, Chem. Mater. 16 (2004) 477.
[6] X. Gao, H. Zhu, G. Pan, S. Ye, Y. Lan, F. Wu, D. Song, J. Phys. Chem. B 108 (2004) 2868.
[7] Z.W. Zhao, Z.P. Guo, D. Wexler, Z.F. Ma, X. Wu, H.K. Liu, Electrochem. Commun. 9 (2007) 697.
[8] B.L. He, B. Dong, H.L. Li, Electrochem. Commun. 9 (2007) 425.
[9] R. Ma, Y. Bando, T. Sasaki, Chem. Phys. Lett. 380 (2003) 577.
[10] S.H. Lim, J. Luo, Z. Zhong, W. Ji, J. Lin, Inorg. Chem. 44 (2005) 4124–4126.
[11] D.V. Bavykim, A.A. Lapkin, P.K. Plucinski, J.M. Friedrich, F.C. Walsh, J. Phys. Chem. B 109 (2005) 19422–19427.
[12] J. Yang, Z. Jin, X. Wang, W. Li, J. Zhang, S. Zhang, X. Guo, Z. Zhang, Chem. Soc., Dalton Trans. (2003) 3898.
[13] M. Zhang, Z. Jin, J. Zhang, X. Guo, J. Yang, W. Ki, X. Wang, Z. Zhang, Mol. Catal. A: Chem. 217 (2004) 203.
[14] G.H. Du, Q. Chen, R.C. Che, Z.Y. Yuan, L.M. Peng, Appl. Phys. Lett. 79 (2001) 3702.
[15] D.H. Kim, Y.H. Jung, D.K. Choi, S.J. Kim, K.S. Lee, J. Nanosci. Nanotechnol. 8 (2008) 1–4.
[16] M. Newville, J. Synchrotron Rad. 8 (2001) 322.
[17] Q. Chen, W.Z. Zhou, G.H. Du, L.M. Peng, Adv. Mater. 14 (2002) 1208.
[18] A.R. Armstrong, G. Armstrong, J. Canales, P.G. Bruce, Angew. Chem., Int. Ed. 43 (2004) 2286.
[19] N. Wang, H. Lin, J.B. Li, X.Z. Yang, B. Chi, C.F. Lin Jr., Alloys Compd. 424 (2006) 311.
[20] X.M. Sun, Y.D. Li, Chem. Eur. J. 9 (2003) 2229.
[21] W.B. Kim, S.H. Choi, J.S. Lee, J. Phys. Chem. B (2000) 8670, 204, 36.
[22] K. Fukuda, I. Nakai, C. Oishi, M. Nomura, M. Harada, Y. Yasuo, T. Sasaki, J. Phys. Chem. B 108 (2004) 13088.
[23] H.C. Choi, H.-Y. Ahn, Y.M. Jung, M.K. Lee, H.J. Shin, S.B. Kim, Y.-E. Sung, Appl. Spectrosc. 58 (2004) 598.
[24] A.N. Mansour, C.A. Melendres, Physica B 208 and 209 (1995) 583.
[25] D.H. Kim, Y.H. Jung, D.K. Choi, S.J. Kim, K.S. Lee, J. Nanosci. Nanotech. 9 (2009) 941.